Robotica (2015) volume 33, pp. 1471–1490. © Cambridge University Press 2014
doi:10.1017/S0263574714000800

An adaptive force reflection scheme for bilateral teleoperation

Zhang Chen†,‡,§, Bin Liang†,§, Tao Zhang†,‡,*, Bo Zhang§ and Haitao Song†

†*Department of Automation, School of Information Science and Technology, Tsinghua University, Beijing 10084, China*
‡*Key Laboratory of Advanced Control and Optimization for Chemical Processes, Shanghai 200237, China*
§*Shenzhen Research Institute, The Chinese University of Hong Kong, Shenzhen 518057, China*

(Accepted March 5, 2014. First published online: April 9, 2014)

SUMMARY
In this paper, an adaptive force reflection scheme is proposed for bilateral teleoperation. In order to achieve an ideal telepresence performance while keeping the system stable, the force reflection algorithm needs to take both the human force and the contact force into consideration. An observer based on the feature of the human operator is designed to estimate the force applied on the master device. The reflected force is calculated by performing the orthogonal decomposition of the contact force, and is adjusted adaptively according to the estimated human force. The direction of the reflected force becomes a key consideration in the design process, so the proposed approach has an advantage in the guiding contact task. Based on the small gain theorem, the master device with the force reflection scheme is proved to be input-to-output stable, and the derivation for stability criterion of the closed-loop teleoperation system is also given. The results of simulations and experiments on a 6-degree of freedom teleoperation system demonstrate the effectiveness of the proposed scheme.

KEYWORDS: Bilateral teleoperation; Force feedback; Stability analysis; Telepresence.

1. Introduction

Telerobotics has become increasingly popular in various fields, such as nuclear research, space exploration, micromanipulation or minimally invasive surgery, underwater vehicles, and so on.[1,2] Force-reflecting teleoperation can provide the human operator with contact force information and thus greatly enhances the operation performance when doing complex tasks. An ideal force-reflecting mechanism is supposed to provide the operator with natural feelings and proper feedback forces.[3] Unfortunately, due to the stability problem of teleoperation systems, it is still one of the main challenges researchers face at present.

The stability problem of bilateral teleoperation has been a highly active research field during the past two decades.[4,5] The time delays existing in the communication channels are the main factors that affect the stability of teleoperators.[6] The passivity-based approaches are the most widely used methods for solving the stability problem brought by time delays. The most popular techniques are the scattering approach proposed by Anderson and Spong,[7] and the wave variables proposed by Niemeyer and Slotine.[8] There are also other controllers designed to stabilize the time-delay teleoperation systems, such as sliding mode control[9] and H_∞ control.[10,11] For more information, the readers may refer to the survey.[12]

Besides the time delay, the reflected forces in bilateral teleoperation also affect the system stability. Daniel and McAree[13] first discussed this issue in detail. They analyzed reflected forces based on their

* Corresponding author. E-mail: taozhang@mail.tsinghua.edu.cn

frequencies. The high frequency parts convey the information needed by the operator, and the low frequency parts are responsible for energetic interactions between the environment and slave robots. Daniel and McAree claimed that there was an upper bound for the reflected force in order to guarantee stability, and they derived some simple criterions for a 1-degree of freedom (DOF) telerobot model. Daniel and McAree's work is very instructive and suggests that there is a balance between the force reflection gain and system stability.

Kuchenbecker and Niemeyer[14] analyzed reflected and control signals in frequency domain and pointed out that the high frequency position commands would lead to the so-called induced master motion (IMM), which causes instability in teleoperation and should be avoided. Kuchenbecker and Niemeyer[14] used an induced motion model to cancel the high frequency motion commands. The model was obtained by identifying each element that connected the user to the controller. In Kuchenbecker and Niemeyer's[14] work, the human–master interaction was also assumed to be a combination of the second-order linear spring-damping systems. Polushin *et al.*[15] relaxed restrictions on the human–master interaction model. In their approach, no particular dynamic model was used. Instead, only some general assumptions were proposed about the movements of the human operator. Specifically, Polushin *et al.*[15] made an assumption that human actions lie in a neighborhood of passivity-based stabilizing control actions. Indeed, such an assumption is reasonable considering that human operators usually tend to stabilize the master manipulators. However, in most cases, it is very difficult for the passivity-based stabilizing control scheme, such as the assumption in Polushin *et al.*,[15] to be always guaranteed during the whole operating process, especially when the operator actively changes the motion of the master manipulator. The assumption consequently limits the application of the force reflection algorithm.

There are generally two kinds of contact tasks in bilateral teleoperation. In the first type the contact force needs to be regulated to finish some tasks, such as cutting materials, tightening the screws, and so on. The other type is that the contact itself is not a task, but it is mainly to provide guidance during the mission. For example, in the docking or plugging task, there is a concave structure around the docking assembly. If the end-effector fails to aim the target, it will contact the concave surface. The contact force can help the operator to adjust the commands and accomplish the mission. In this situation, we could call it the guiding contact task. In the first type of task, the magnitude of the reflected force is critical for haptic realism.[16] On the other hand, in the guiding contact task, the direction of the reflected force plays an important role. Drifts in reflection direction may lead to mission failures. Recently, great interest has been shown in force direction in the field of haptic rending.[17,18] However, in the area of bilateral control, the importance of force-reflecting direction is often neglected because of the trade-off between stability and telepresence. For example, in Kuchenbecker *et al.*'s approach,[14,16] the reflected force cannot represent the true direction of the contact force (the reason will be analyzed later). Due to the importance of direction in teleoperation (especially in guiding contact task), direction of the force will be emphasized when designing the reflection scheme in this work.

In this paper, the force reflection mechanism is studied. Section 2 proposes the adaptive force reflection scheme. First a human force estimation algorithm is designed. Using this estimated force and several novel concepts, an adaptive force reflecting algorithm is then proposed based on the orthogonal decomposition of the contact force. Section 3 analyzes the performance of the force reflection scheme, including stability and telepresence. The convergence of the estimation errors is derived. By utilizing the multichannel input-to-output stable (IOS) small gain theorem, stability of the time-delay force-reflecting teleoperation is proved. The haptic experience of the proposed method is analyzed from the magnitude and the direction of the reflected force. In Section 4, simulations and experiments are carried out to verify the performance of the proposed force reflection scheme. The experiment results demonstrate the effectiveness of the algorithm. Section 5 is the conclusion of this paper.

Notation. *Some functional conceptions*[19] *are used in the following discussion. A continuous function* $\gamma : \mathbb{R}^+ \to \mathbb{R}^+$ *is said to belong to class* $\mathcal{G}$ *if* $\gamma(0) = 0$ *and* $\gamma(x) \geq \gamma(y),\ \forall x > y \geq 0$. *A function* γ *belongs to class* $\mathcal{K}$ *if* $\gamma \in \mathcal{G}$ *and* γ *is strictly increasing. A function belongs to class* $\mathcal{K}_\infty$ *if* $\gamma \in \mathcal{K}$ *and* $\gamma(x) \to \infty$ *as* $x \to \infty$. *A continuous function* $\beta : \mathbb{R}^+ \times \mathbb{R}^+ \to \mathbb{R}^+$ *is said to be of class* $\mathcal{KL}$ *if* $\beta(\cdot, t) \in \mathcal{K},\ \forall t \geq 0$, *and* $\beta(x, \cdot)$ *is monotonically decreasing to zero for each* $x > 0$.[20]

https://doi.org/10.1017/S0263574714000800 Published online by Cambridge University Press

2. Adaptive Force Reflection Scheme

2.1. Estimation of human force

Because bilateral teleoperators belong to human-in-loop systems, the states of a human operator should be taken into account. Since typical haptic hand controllers do not have built-in force sensors, a human force estimator is first designed in this section.

Without loss of generality, the dynamics of master manipulator can be modeled as an Euler–Lagrange form,[21]

$$M(q)\ddot{q} + C(q, \dot{q})\dot{q} + g(q) = \tau_h + \tau_{\mathrm{rf}}, \tag{1}$$

where τ_h and τ_{rf} denote the torques imposed on the joints, mapping from the human force F_h and the reflected force F_{rf}, respectively.

Remark 1. In Eq. (1) the local control torques are not explicitly listed. It can be explained that $M(q)$, $C(q, \dot{q})$, and $g(q)$ in (1) are equivalent inertia matrix, centrifugal and Coriolis force matrix, and gravitational force vector in which the local control torques have already been taken into account.

Before the derivation of the human force estimation algorithm, some assumptions about the master manipulator are made.

Assumption 1. The information of joint position and joint velocity can be obtained, i.e., q and $\dot{q}$ are available when estimating the human force. The measurement noise of $\dot{q}$ is upper-bounded.

Assumption 2. The variation of the human force is assumed to be Lebesgue-measurable, and is bounded by $\sup_{t\geq 0} |\dot{\tau}_h(t)| \leq d$.

The above assumptions are reasonable and suitable for most real systems. Under Assumption 1, the dynamics can be rewritten as

$$\begin{aligned} \frac{d}{dt}(\underbrace{M(q)\dot{q}}_{x(t)}) &= \underbrace{\dot{M}(q)\dot{q} - C(q, \dot{q})\dot{q} - g(q) + \tau_{\mathrm{rf}}}_{u(t)} + \tau_h, \\ z(t) &= M(q)(\dot{q} + \varepsilon(t)), \end{aligned} \tag{2}$$

where $\varepsilon(t)$ is the measurement noise of $\dot{q}$, and $z(t)$ is the observation value of the system.

When estimating the human force, it is necessary to consider the characteristic of human behavior. In Tanner and Niemeyer's work,[22] it is pointed out that human's input–output system is quite asymmetric. Human hands are able to recognize force signals of up to 1 kHz, but can only act under the frequency below 10 Hz. The manipulation of human falls in a typical low frequency bound. Therefore, based on Eq. (2), a straightforward way to estimate the value of τ_h can be proposed as

$$\hat{\tau}_h(s) = \frac{1}{\alpha s + 1}\left(s \cdot z(s) - u(s)\right), \tag{3}$$

where s denotes the Laplacian operator. From (3), it can be seen that there is a low pass component in the estimation process.[23] Define the intermediate signals[24] $\sigma(t)$ and $\zeta(t)$ as

$$\begin{cases} \sigma(s) = -\frac{1}{\alpha^2 s + \alpha} z(s), \\ \zeta(s) = -\frac{1}{\alpha s + 1} u(s). \end{cases} \tag{4}$$

https://doi.org/10.1017/S0263574714000800 Published online by Cambridge University Press

Performing the inverse Laplace transformation on Eqs. (3) and (4), and combining them yield the following human force estimation algorithm:

$$\begin{cases} \hat{\tau}_h(t) = \frac{1}{\alpha} z(t) + \sigma(t) + \zeta(t), \\ \dot{\sigma}(t) = -\frac{1}{\alpha^2} z(t) - \frac{1}{\alpha}\sigma(t), \\ \dot{\zeta}(t) = -\frac{1}{\alpha} u(t) - \frac{1}{\alpha}\zeta(t). \end{cases} \tag{5}$$

2.2. Orthogonal decomposition-based force reflection

A simple way to reflect force is to impose the same force as the contact force in slave side, which can theoretically guarantee the ideal transparency for bilateral teleoperation. In this way the operator is able to feel exactly the same force as the slave robot. Generally, when the environment force becomes too large, the human operator will adjust the haptic device to avoid damaging the slave robot. However, if the environment is with high stiffness, the contact force will change drastically. A direct reflection of the contact force will make it very difficult for the human operator to stabilize the master. In this case the aforementioned IMMs are brought in and the master–slave coupled oscillation will happen, which is not desired in bilateral teleoperation. Therefore, it is necessary that the reflected force should be adjusted based on both environment force and human force.

In this section, the concepts "speed-gradient" or "passivity-based" stabilizing control[25] are used to construct two sets, namely, the passive behavior region and the non-passive behavior region. Accordingly, for further analysis, there are "passive distance" and "passive margin" denoting how far the human operator's action is away from the passive behavior region or the non-passive behavior region. To illustrate the definition of passive behavior and passive distance, the master manipulator system is assumed to be input-to-state stable (ISS).

Assumption 3. Rewrite the dynamics of master manipulator (1) into a more general ordinary differential equation form as,

$$\dot{x}_m = g(x_m) + h(x_m)u_m. \tag{6}$$

System (6) is ISS, i.e., it admits $\underline{\alpha}$, $\bar{\alpha} \in \mathcal{K}_\infty$ such that there exists a smooth storage function $V(x_m(t)) : \mathbb{R}^n \to \mathbb{R}^+$ satisfies[26,27]

$$\underline{\alpha}(|x_m(t)|) \leq V(x_m(t)) \leq \bar{\alpha}(|x_m(t)|), \quad \forall x_m(t) \in \mathbb{R}^n, \tag{7}$$

and there exist some $\alpha_m \in \mathcal{K}_\infty$, $\gamma_m \in \mathcal{K}$ so that

$$\dot{V}(x_m(t)) := \nabla V(x_m(t))\,[g(x_m) + h(x_m)u_m] \leq -\alpha_m(|x_m(t)|) + \gamma_m(|u_m(t)|), \quad \forall x_m(t),\ u_m(t) \in \mathbb{R}^n. \tag{8}$$

There always exist a set of "passivity-based" stabilizing control actions for system (6), which is,[15]

$$\Xi(x_m) := \left\{ \eta \cdot \frac{\partial V}{\partial x_m} h(x_m), \quad \eta \in [-\infty,\ 0] \right\}. \tag{9}$$

Based on the conception of the passivity-based stabilizing control action, the human action space could be divided into passive behavior set Θ and non-passive behavior set $\Theta^\perp$ according to its projection onto the set (9). The concepts of passive margin and passive distance are given as follows.

Definition 1. When the human action falls in the space of passive behavior region Θ, the passive margin $\zeta \in \mathbb{R}^+$ denotes the distance from the action to the non-passive region. For the actions falling in the space of non-passive behavior region $\Theta^\perp$, the passive distance $\psi \in \mathbb{R}^+$ denotes the distance from the action to the passive region.

The reflected force F_r can be a compromise based on the overall analysis of the human force F_h and the contact force F_{env} in the slave side. Indeed, in order to achieve ideal telepresence, the reflected force F_r should be equal to, or at least in proportion to, F_{env} so that the operator can feel the contact

https://doi.org/10.1017/S0263574714000800 Published online by Cambridge University Press

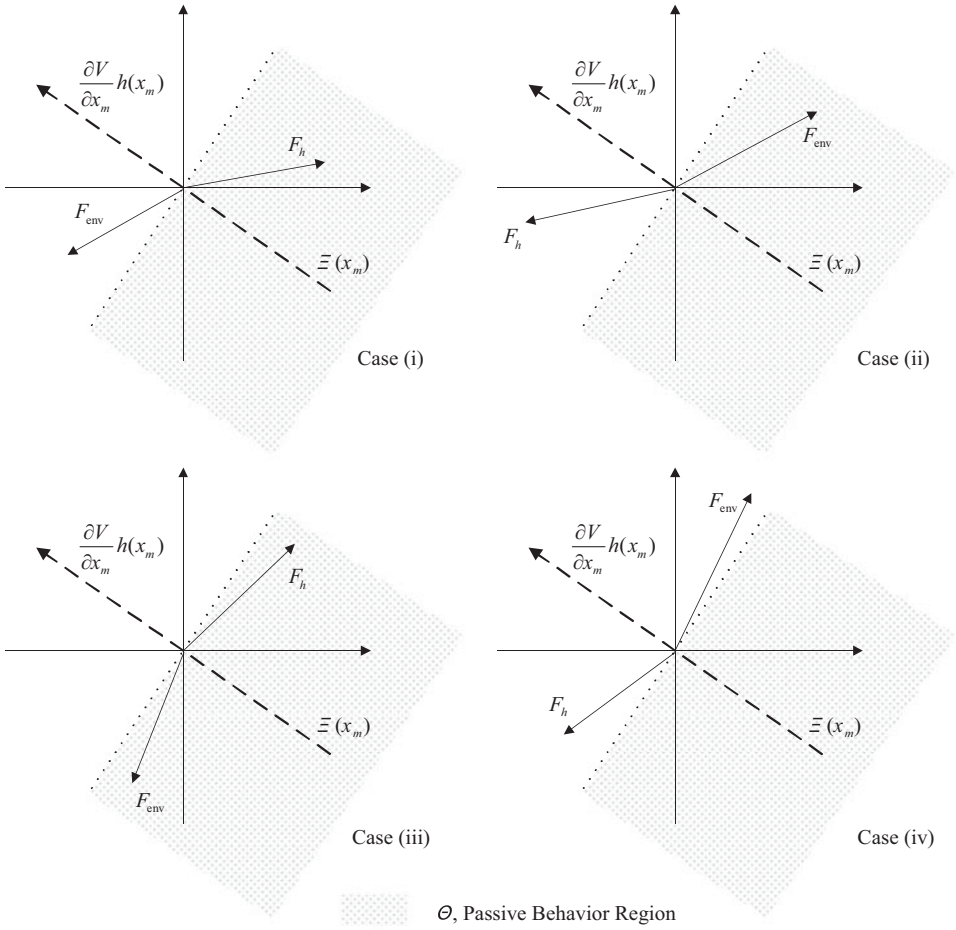

Fig. 1. Four cases of operation.

force being the same as the slave robot. However, for the consideration of stability, both amplitude and direction of F_r cannot be chosen arbitrarily.

There are four combinations for F_h and F_{env} if they are described in the space of passive behavior and non-passive behavior regions, which are as follows:

1. F_h in the passive region, and F_{env} in the non-passive region.
2. F_h in the non-passive region and F_{env} in the passive region.
3. Both F_h and F_{env} in the passive region.
4. Both F_h and F_{env} in the non-passive region.

Remark 2. In this paper, we only consider the situations when the human force and the contact force are basically along opposite directions, i.e., $F_h^T F_{\text{env}} \leq 0$. If $F_h^T F_{\text{env}} > 0$, it means that the human force actually pushes the robot in the same direction as done by the contact force. In this case, the reflection force should be switched off completely or be applied on the master device with a very low gain to guarantee the overall stability.[28]

Remark 3. If F_h and F_{env} are exactly in the same line, i.e., the angle between the two forces is π, then there will be only case (i) and case (ii). Most of the existing researches merely study the above two cases. However, it should be noted that in most cases F_h and F_{env} are not collinear, therefore both cases (iii) and (iv) are possible in real applications. Figure 1 illustrates the examples of the four cases.

It will bring much convenience to analyze the stability of teleoperation in the subspaces spanned by $\Xi(x_m)$ and its orthogonal complement $\Xi^{\perp}(x_m)$. Define the orthogonal projections of environment force onto the two subspaces as F_{env}^{Ξ} and $F_{\text{env}}^{\perp\Xi}$, and define $\bar{F}_h$ to be the estimation of F_h. Through orthogonal decomposition, both forces F_{env} and $\bar{F}_h$ are divided into two parts. The projections on

https://doi.org/10.1017/S0263574714000800 Published online by Cambridge University Press

subspace $\Xi(x_m)$ are related to stability, while the orthogonal complement parts have no effect on system stability. When designing the force reflection algorithm, the projection on $\Xi(x_m)$ is considered in the first place to keep the teleoperators stable. After the system stability is guaranteed, the part of $F_{\text{env}}^{\perp\Xi}$ needs to be adjusted to obtain a desired telepresence performance. To be more specific, the four cases are discussed separately.

Case (i) In this case, the reflection of F_{env}^{Ξ} may cause stability problem. However, the human force belongs to region Θ and hence is a stabilizing input. Therefore, the reflection of F_{env}^{Ξ} is based on the comparison between the magnitude of F_{env}^{Ξ} and $\bar{F}_h^{\Xi}$. If $|F_{\text{env}}^{\Xi}|$ is smaller than $|\bar{F}_h^{\Xi}|$, the reflected force is determined by F_{env}^{Ξ}, otherwise the magnitude of F_r will be determined by $|\bar{F}_h^{\Xi}|$ to maintain the stability of the system. As mentioned before, after the reflection of F_{env}^{Ξ} is fixed, the reflection of $F_{\text{env}}^{\perp\Xi}$ needs to be adjusted. In this scheme, the principle of adjusting is to reproduce the same direction in the reflection force as F_{env}.

Cases (ii) and (iii) In both cases, the reflection of F_{env} is a stabilizing input. Hence, the reflecting gain could be chosen independent of $\bar{F}_h$.

Case (iv) In this case, both $\bar{F}_h$ and F_{env}^{Ξ} are unstabilizing inputs. The reflection of F_{env} depends on the comparison between $|F_{\text{env}}^{\Xi}|$ and $|\bar{F}_h^{\Xi}|$. If $|\bar{F}_h^{\Xi}|$ is big, then $|F_{\text{env}}^{\Xi}|$ should be small and *vice versa*.

According to above analysis, a force reflection scheme based on the orthogonal decomposition of F_{env} is proposed as the following formula:

$$F_r = \begin{cases} \chi_1\left(\left|\bar{F}_h^{\Xi}\right| \text{Sat}\left(\left|F_{\text{env}}^{\Xi}\right|/\left|\bar{F}_h^{\Xi}\right|\right)\right)\frac{\bar{F}_h^{\Xi}}{|F_h^{\Xi}|} & \\ \quad + \frac{\chi_1(|\bar{F}_h^{\Xi}|\text{Sat}(|F_{\text{env}}^{\Xi}|/|\bar{F}_h^{\Xi}|))}{|F_{\text{env}}^{\Xi}|} F_{\text{env}}^{\perp\Xi} & \bar{F}_h \in \Theta, \quad F_{\text{env}} \in \Theta^{\perp} \\ \chi_2(|F_{\text{env}}|)\frac{F_{\text{env}}}{|F_{\text{env}}|} & \bar{F}_h \in \Theta, \quad F_{\text{env}} \in \Theta, \\ \chi_3(|F_{\text{env}}|)\frac{F_{\text{env}}}{|F_{\text{env}}|} & \bar{F}_h \in \Theta^{\perp}, \ F_{\text{env}} \in \Theta \\ \frac{\chi_4(|\bar{F}_h^{\Xi}|\text{Sat}(|F_{\text{env}}^{\Xi}|/|\bar{F}_h^{\Xi}|))}{|F_{\text{env}}^{\Xi}|} F_{\text{env}} & \bar{F}_h \in \Theta^{\perp}, \ F_{\text{env}} \in \Theta^{\perp} \end{cases} \tag{10}$$

where $\chi_i : \mathbb{R}^+ \to \mathbb{R}^+$ is a continuous function satisfying $\chi_i(\cdot) \in \mathcal{G}$, and $\text{Sat}(\cdot) : \mathbb{R}^+ \to \mathbb{R}^+$ is a saturation function, which is used in the comparison of $|F_{\text{env}}^{\Xi}|$ and $|\bar{F}_h^{\Xi}|$. The saturation function ensures that the variable of $\chi_i(\cdot)$ is not greater than $|\bar{F}_h^{\Xi}|$; otherwise stability issues will arise. The saturation function is specified by

$$\text{Sat}(x) = \begin{cases} x & x \in [0, \ 1) \\ 1 & x \in [1, \ +\infty) \end{cases}. \tag{11}$$

The principle of algorithm (10) is that when the system does not tend to unstable, telepresence becomes the primary concern; otherwise the reflected force should first satisfy the stability condition. For example, if the contact force belongs to the passive region, then the force reflection gain can be higher. Some IMM might arise, but in this case the stability will not be affected. If the contact force falls in the non-passive region, then the reflection gain should be chosen very carefully. Zero drift in the direction of the reflected force could be guaranteed during bilateral teleoperation. This is another feature of algorithm (10). As is stated in Section 1, in the guiding contact task, the information of the force direction is an important factor in haptic experience.

Remark 4. In the previous researches, the direction information of the contact force was changed to avoid IMMs, which were considered as the main factor causing instability in force-reflecting teleoperation.[14,15] However, not all IMMs bring instability. Overemphasis of eliminating IMMs will sacrifice some useful feedback information about the contact direction.

https://doi.org/10.1017/S0263574714000800 Published online by Cambridge University Press

3. Performance Analysis

3.1. Estimate error convergence

The following theorem is about the errors and convergence of the human force estimation algorithm.

Theorem 1. Consider the human–master manipulator interaction system described by dynamics (2) under Assumptions 1 and 2, and in addition if either of the following two conditions can be satisfied:

1. The joint velocity measurement error $\varepsilon(t)$ is upper-bounded such that $\sup_{t\geq 0}|\varepsilon(t)| \leq \xi_1$;
2. The variation of $\varepsilon(t)$ is the Lebesgue-measurable function and $\sup_{t\geq 0}|\dot{\varepsilon}(t)| \leq \xi_2$;

then the errors of the human force estimating (5) are bounded as $t \to \infty$. More specifically, under the condition 1, it admits $\beta_1 \in \mathcal{KL}$, $\gamma_1^{(\varepsilon)} \in \mathcal{K}$, $\gamma_1^{(\tau)} \in \mathcal{K}$, such that

$$|\hat{\tau}_h - \tau_h| \leq \max\left\{\beta_1\left(|\hat{\tau}_h(0) - \tau_h(0)|, t\right), \gamma_1^{(\varepsilon)}\left(\sup_{t>0}|\bar{\varepsilon}(t)|\right), \gamma_1^{(\tau)}\left(\sup_{t\geq 0}|\dot{\tau}_h(t)|\right)\right\}, \tag{12}$$

and under the condition 2, it admits $\beta_2 \in \mathcal{KL}$, $\gamma_2^{(\varepsilon)} \in \mathcal{K}$, $\gamma_2^{(\tau)} \in \mathcal{K}$, such that

$$|\hat{\tau}_h - \tau_h| \leq \max\left\{\beta_2\left(|\hat{\tau}_h(0) - \tau_h(0)|, t\right), \gamma_2^{(\varepsilon)}\left(\sup_{t>0}|\dot{\bar{\varepsilon}}(t)|\right), \gamma_2^{(\tau)}\left(\sup_{t\geq 0}|\dot{\tau}_h(t)|\right)\right\}. \tag{13}$$

Proof: Cases (i) and (ii) are discussed respectively.

Case (i). Set $\tilde{\tau}_h(t) = \frac{1}{\alpha}x(t) + \sigma(t) + \zeta(t)$. The relationship between $\tilde{\tau}_h(t)$ and $\hat{\tau}_h(t)$ is easy to obtain:

$$\tilde{\tau}_h(t) = \hat{\tau}_h(t) - \frac{1}{\alpha}M(q)\varepsilon(t). \tag{14}$$

Use the property of the inertia matrices that $M(q)$ is uniformly positive definite with lower and upper bounds,

$$0 < \lambda_{\min}\{M_i(q_i)\}I \leq M_i(q_i) \leq \lambda_{\max}\{M_i(q_i)\}I < \infty. \tag{15}$$

Defining $\bar{\varepsilon}(t)$ as $\bar{\varepsilon}(t) = M(q)\varepsilon(t)$, and combining condition (i), it can be concluded that there exists a $\bar{\xi}_1$ such that $\sup_{t\geq 0}|\bar{\varepsilon}(t)| \leq \bar{\xi}_1$.

Let $V = \frac{1}{2}(\tilde{\tau}_h - \tau_h)^2$. Differentiating V with respect to time t gives

$$\begin{aligned}
\dot{V} &= \left[\frac{1}{\alpha}(u(t) + \tau_h) + \left(-\frac{1}{\alpha^2}z(t) - \frac{1}{\alpha}\sigma(t)\right) + \left(-\frac{1}{\alpha}u(t) - \frac{1}{\alpha}\zeta(t)\right) - \dot{\tau}_h\right](\tilde{\tau}_h - \tau_h) \\
&= \left(\frac{1}{\alpha}(\tau_h - \tilde{\tau}_h) - \frac{1}{\alpha^2}M(q)\varepsilon(t) - \dot{\tau}_h\right)(\tilde{\tau}_h - \tau_h) \\
&= -\frac{1}{\alpha}(\tilde{\tau}_h - \tau_h)^2 + \left(-\frac{1}{\alpha^2}\bar{\varepsilon}(t) - \dot{\tau}_h\right)(\tilde{\tau}_h - \tau_h) \\
&\leq -\frac{1}{\alpha}V(t) + \frac{\alpha}{2}\left(\frac{1}{\alpha^2}\bar{\varepsilon}(t) + \dot{\tau}_h(t)\right)^2.
\end{aligned} \tag{16}$$

Using the fact that $\dot{V} \leq -aV + b \Rightarrow V(t) \leq e^{-\mathrm{at}}V(0) + \frac{b}{a}$, the upper bound of $V(t)$ can be derived as

$$V(t) \leq e^{-\frac{t}{\alpha}}V(0) + \frac{\alpha^2}{2}\left(\frac{1}{\alpha^2}\bar{\varepsilon}(t) + \sup_{t\geq 0}|\dot{\tau}_h(t)|\right)^2 \leq e^{-\frac{t}{\alpha}}V(0) + \frac{\alpha^2}{2}\left(\frac{1}{\alpha^2}\bar{\xi}_1 + d\right)^2. \tag{17}$$

https://doi.org/10.1017/S0263574714000800 Published online by Cambridge University Press

The error between $\tilde{\tau}_h$ and τ_h is bounded as

$$|\tilde{\tau}_h - \tau_h| \leq \sqrt{2e^{-\frac{t}{\alpha}} V(0) + \alpha^2 \left(\frac{1}{\alpha^2}\bar{\xi}_1 + d\right)^2}. \tag{18}$$

Recalling Eq. (14), it could be concluded that $|\hat{\tau}_h - \tau_h|$ is bounded in $[-(\frac{2}{\alpha}\xi + \alpha d), \frac{2}{\alpha}\xi + \alpha d]$ as $t \to \infty$.

From inequality (17), the upper bound of $(\tilde{\tau}_h(t) - \tau_h(t))^2$ can be expressed in a more general form,

$$(\tilde{\tau}_h(t) - \tau_h(t))^2 \leq \max\left\{2e^{-\frac{t}{\alpha}} \left(\tilde{\tau}_h(0) - \tau_h(0)\right)^2, \alpha^2 \left(\frac{1}{\alpha^2}\bar{\varepsilon}(t) + \sup_{t\geq 0}|\dot{\tau}_h(t)|\right)\right\}, \tag{19}$$

which implies that there exist appropriate gains $\tilde{\beta}_1$, $\tilde{\gamma}_1^{\varepsilon}$, and $\tilde{\gamma}_1^{\tau}$, such that

$$|\tilde{\tau}_h - \tau_h| \leq \max\left\{\tilde{\beta}_1\left(|\tilde{\tau}_h(0) - \tau_h(0)|, t\right), \tilde{\gamma}_1^{(\varepsilon)}\left(\sup_{t>0}|\bar{\varepsilon}(t)|\right), \tilde{\gamma}_1^{(\tau)}\left(\sup_{t\geq 0}|\dot{\tau}_h(t)|\right)\right\}. \tag{20}$$

Using the fact that $|\tilde{\tau}_h - \tau_h| = |\hat{\tau}_h - \tau_h - \bar{\varepsilon}(t)|$, it can be derived that

$$\begin{aligned} |\hat{\tau}_h - \tau_h| &\leq |\tilde{\tau}_h - \tau_h| + \sup_{t>0}|\bar{\varepsilon}(t)| \\ &\leq \max\left\{\beta_1\left(|\tilde{\tau}_h(0) - \tau_h(0)|, t\right), \gamma_1^{(\varepsilon)}\left(\sup_{t>0}|\bar{\varepsilon}(t)|\right), \gamma_1^{(\tau)}\left(\sup_{t\geq 0}|\dot{\tau}_h(t)|\right)\right\}. \end{aligned} \tag{21}$$

Case (ii). Under this condition, choose $V(t)$ as $V = \frac{1}{2}(\hat{\tau}_h - \tau_h)^2$, then the derivative of $V(t)$ with respect to time t is

$$\begin{aligned} \dot{V} &= (\hat{\tau}_h - \tau_h)\left(\dot{\hat{\tau}}_h - \dot{\tau}_h\right) \\ &= (\hat{\tau}_h - \tau_h)\left[\frac{1}{\alpha}\left(u(t) + \tau_h + \dot{\bar{\varepsilon}}(t)\right) + \left(-\frac{1}{\alpha^2}z(t) - \frac{1}{\alpha}\sigma(t)\right) + \left(-\frac{1}{\alpha}u(t) - \frac{1}{\alpha}\zeta(t)\right) - \dot{\tau}_h\right] \\ &= (\hat{\tau}_h - \tau_h)\left(\frac{1}{\alpha}\tau_h - \frac{1}{\alpha}\hat{\tau}_h + \frac{1}{\alpha}\dot{\bar{\varepsilon}}(t) - \dot{\tau}_h\right) \\ &= -\frac{1}{\alpha}(\hat{\tau}_h - \tau_h)^2 + (\hat{\tau}_h - \tau_h)\left(\frac{1}{\alpha}\dot{\bar{\varepsilon}}(t) - \dot{\tau}_h\right) \\ &\leq -\frac{1}{2\alpha}(\hat{\tau}_h - \tau_h)^2 + \frac{\alpha}{2}\left(\frac{1}{\alpha}\dot{\bar{\varepsilon}}(t) - \dot{\tau}_h\right)^2. \end{aligned} \tag{22}$$

Similar to case (i), there exists a $\bar{\xi}_2$ such that $\sup_{t\geq 0}|\dot{\bar{\varepsilon}}(t)| \leq \bar{\xi}_2$. $V(t)$ is upper-bounded by

$$V(t) \leq e^{-\frac{1}{\alpha}t} V(0) + \frac{\alpha^2}{2}\left(\frac{1}{\alpha}\bar{\xi}_2 + d\right)^2. \tag{23}$$

Therefore, the estimation error $|\hat{\tau}_h - \tau_h|$ is bounded in $[-\frac{1}{\sqrt{2}}(\bar{\xi}_2 + \alpha d), \frac{1}{\sqrt{2}}(\bar{\xi}_2 + \alpha d)]$ as $t \to \infty$.

Also, the existence of $\tilde{\beta}_2$, $\tilde{\gamma}_2^{(\varepsilon)}$, and $\tilde{\gamma}_2^{(\tau)}$ in inequality (13) could be proved as in case (i).

3.2. System stability

In this section, the stability of the master subsystem and the closed-loop teleoperation system will be studied. First, a lemma is introduced, which is about the stability of the subsystem with input as the estimated force $\bar{F}_h$.

https://doi.org/10.1017/S0263574714000800 Published online by Cambridge University Press

Lemma 1. Consider the following subsystem,

$$\begin{cases} \dot{x}_m = g(x_m) + h(x_m)(\bar{F}_h + F_r), \\ F_r = f_r(\bar{F}_h, F_{\text{env}}), \end{cases} \tag{24}$$

where $f_r(\cdot)$ is given by (10). There exists $\chi^* \in \mathcal{K}_\infty$ such that if $\max\{\chi_1(s), 2\chi_4(s)\} \leq \chi^*(s)$ holds for all $s \geq 0$, then system (24) is ISS with states x_m and inputs $\{\bar{\zeta}_h, \bar{\psi}_h, F_{\text{env}}\}$, where $\bar{\zeta}_h$ and $\bar{\psi}_h$ are the passive margin and distance of the estimated human action in the sense of Definition 1 respectively.

Proof. Assumption 1 has implied that the master device admits a continuously differentiable function $V_m : \mathbb{R}^n \to \mathbb{R}^+$ satisfies (7) and (8) for some $\underline{\alpha}$, $\bar{\alpha}$, $\alpha_m \in \mathcal{K}_\infty$ and $\gamma \in \mathcal{K}$. Choose V_m as the ISS Lyapunov function, and the time derivative of V_m is

$$\dot{V}(x_m(t)) := \nabla V(x_m(t)) \left[g(x_m) + h(x_m)(\bar{F}_h + F_r) \right]. \tag{25}$$

It can be derived from (8) that

$$\nabla V(x_m(t)) g(x_m) \leq -\alpha_m(|x_m(t)|) \ \ \forall x_m(t) \in \mathbb{R}^n. \tag{26}$$

The property of $\nabla V(x_m(t))[g(x_m) + h(x_m)(\bar{F}_h + F_r)]$ will be analyzed in the following steps
(i) $\bar{F}_h \in \Theta, \quad F_{\text{env}} \in \Theta^\perp$

$$\begin{aligned} &\nabla V(x_m(t))[g(x_m) + h(x_m)(\bar{F}_h + F_r)] = \nabla V(x_m(t)) g(x_m) + \nabla V(x_m(t)) h(x_m) \\ &\times \left(\bar{F}_h - \chi_1 \left(\left| \bar{F}_h^\Xi \right| \text{Sat} \left(\left| F_{\text{env}}^\Xi \right| / \left| \bar{F}_h^\Xi \right| \right) \right) \frac{\bar{F}_h^\Xi}{\left| F_h^\Xi \right|} + \frac{\chi_1 \left(\left| \bar{F}_h^\Xi \right| \text{Sat} \left(\left| F_{\text{env}}^\Xi \right| / \left| \bar{F}_h^\Xi \right| \right) \right)}{\left| F_{\text{env}}^\Xi \right|} F_{\text{env}}^{\perp\Xi} \right). \end{aligned} \tag{27}$$

If $|F_{\text{env}}^\Xi| \geq |\bar{F}_h^\Xi|$, it can be derived that

$$\nabla V(x_m(t)) h(x_m)(\bar{F}_h + F_r) = \nabla V(x_m(t)) h(x_m) \left(\bar{F}_h - \chi_1 \left(\left| \bar{F}_h^\Xi \right| \right) \bar{F}_h^\Xi / \left| \bar{F}_h^\Xi \right| \right). \tag{28}$$

Now consider the function $[\chi_1 - \mathbb{I}](\cdot)$, where $\mathbb{I}(\cdot) : \mathbb{R}^+ \to \mathbb{R}^+$ is the identify function, i.e., $\mathbb{I}(x) = x$ for all $x \geq 0$. If $[\chi_1 - \mathbb{I}](\cdot) \in \mathcal{G}$ then we have

$$\begin{aligned} &\nabla V(x_m(t)) g(x_m) + \nabla V(x_m(t)) h(x_m) \left(\bar{F}_h - \chi_1 \left(\left| \bar{F}_h^\Xi \right| \right) \bar{F}_h^\Xi / \left| \bar{F}_h^\Xi \right| \right) \\ &= \nabla V(x_m(t)) g(x_m) + \nabla V(x_m(t)) h(x_m) \left((\mathbb{I} - \chi_1) \left(\left| \bar{F}_h^\Xi \right| \right) \bar{F}_h^\Xi / \left| \bar{F}_h^\Xi \right| \right) \\ &\leq -\alpha_m(|x_m(t)|) + \gamma \circ (\chi_1 - \mathbb{I})(\zeta_h), \end{aligned} \tag{29}$$

where $\bar{\zeta}_h$ is the passive margin of the estimated human action. Otherwise, if $[\chi_1 - \mathbb{I}](\cdot) \notin \mathcal{G}$, since $\chi_1 \in \mathcal{G}$, it is straightforward that

$$\nabla V(x_m(t)) g(x_m) + \nabla V(x_m(t)) h(x_m) \left(\bar{F}_h - \chi_1 \left(\left| \bar{F}_h^\Xi \right| \right) \bar{F}_h^\Xi / \left| \bar{F}_h^\Xi \right| \right) \ \leq -\alpha_m(|x_m(t)|) \tag{30}$$

If $\left| F_{\text{env}}^\Xi \right| < \left| \bar{F}_h^\Xi \right|$, (28) can be rewritten as

$$\nabla V(x_m(t)) h(x_m)(\bar{F}_h + F_r) = \nabla V(x_m(t)) h(x_m) [\bar{F}_h + \chi_1 (|F_{\text{env}}|) F_{\text{env}} / |F_{\text{env}}|]. \tag{31}$$

Also, depending on whether the function $[\chi_1 - \mathbb{I}](\cdot)$ belongs to $\mathcal{G}$ or not, the upper bound of (27) can be given as

$$\begin{aligned} &\nabla V(x_m(t)) g(x_m) + \nabla V(x_m(t)) h(x_m)(\bar{F}_h + F_r) \\ &= \nabla V(x_m(t)) g(x_m) + \nabla V(x_m(t)) h(x_m) \left(\bar{F}_h + \chi_1 \left(\left| F_{\text{env}}^\Xi \right| \right) F_{\text{env}}^\Xi / \left| F_{\text{env}}^\Xi \right| + \chi_1 \left(\left| F_{\text{env}}^{\perp\Xi} \right| \right) F_{\text{env}}^{\perp\Xi} / \left| F_{\text{env}}^{\perp\Xi} \right| \right) \end{aligned} \tag{32}$$

https://doi.org/10.1017/S0263574714000800 Published online by Cambridge University Press

$$\leq \begin{cases} -\alpha_m(|x_m(t)|), & \text{if } [\chi_1 - \mathbb{I}](\cdot) \notin \mathcal{G} \\ -\alpha_m(|x_m(t)|) + \gamma\left(\max(\bar{\zeta}_h,\ \chi_1\,|F_{\text{env}}|)\right), & \text{if} [\chi_1 - \mathbb{I}](\cdot) \in \mathcal{G} \end{cases}.$$

(ii) $F_h \in \Theta,\ F_{\text{env}} \in \Theta$
Using (10) and calculating $\dot{V}(x_m(t))$, yield

$$\begin{aligned} &\nabla V(x_m(t))[g(x_m) + h(x_m)(\bar{F}_h + F_r)] \\ &\quad = \nabla V(x_m(t))g(x_m) + \nabla V(x_m(t))h(x_m)\left(\bar{F}_h + \chi_2\,(|F_{\text{env}}|)\,\frac{F_{\text{env}}}{|F_{\text{env}}|}\right) \\ &\quad \leq -\alpha_m(|x_m(t)|). \end{aligned} \tag{33}$$

(iii) $F_h \in \Theta^{\perp},\ F_{\text{env}} \in \Theta$ Since the human action falls in the non-passive region, denoting the passive distance of human action as ψ_h, we have

$$\begin{aligned} &\nabla V(x_m(t))\left[g(x_m) + h(x_m)(\bar{F}_h + F_r)\right] \\ &\quad = \nabla V(x_m(t))g(x_m) + \nabla V(x_m(t))h(x_m)\left(\bar{F}_h + \chi_3(|F_{\text{env}}|)\frac{F_{\text{env}}}{|F_{\text{env}}|}\right) \\ &\quad \leq -\alpha_m(|x_m(t)|) + \nabla V(x_m(t))h(x_m)\left(\bar{F}_h^{\Xi}\right) \\ &\quad \leq -\alpha_m(|x_m(t)|) + \gamma(\bar{\psi}_h). \end{aligned} \tag{34}$$

(iv) $F_h \in \Theta^{\perp},\ F_{\text{env}} \in \Theta^{\perp}$
In this case, both human action and environment force fall in the non-passive region. The time derivative of the ISS Lyapunov function is

$$\begin{aligned} &\nabla V(x_m(t))\left[g(x_m) + h(x_m)(\bar{F}_h + F_r)\right] \\ &\quad = \nabla V(x_m(t))g(x_m) + \nabla V(x_m(t))h(x_m)\left(\bar{F}_h + \chi_4(|F_{\text{env}}|)\frac{F_{\text{env}}}{|F_{\text{env}}|}\right) \\ &\quad \leq -\alpha_m(|x_m(t)|) + L_G V_m\left(\bar{F}_h^{\Xi} + \chi_4(|F_{\text{env}}|)F_{\text{env}}^{\Xi}\big/\left|F_{\text{env}}^{\Xi}\right|\right) \\ &\quad \leq -\alpha_m(|x_m(t)|) + \gamma(\max(2\bar{\psi}_h, 2\chi_4(|F_{\text{env}}|))). \end{aligned} \tag{35}$$

Inequalities (29), (30), (32), (33), (34), and (35) can be rewritten in the following general form:

$$\nabla V(x_m(t))\left[g(x_m) + h(x_m)(\bar{F}_h + F_r)\right] \leq -\alpha_m(|x_m(t)|) + \gamma_m(\max(\bar{\zeta}_h, 2\bar{\psi}_h, \chi^*(|F_{\text{env}}|))), \tag{36}$$

where $\chi^* = \max\{\chi_1, 2\chi_4\}$.

There are switches between the control laws, whose effect on system stability also needs to be analyzed. Here some conclusions in switched nonlinear systems are utilized. Denote $\sigma = \{1,\ 2,\ 3,\ 4\}$ as the index set. Consider $\{\bar{\zeta}_h, 2\bar{\psi}_h, \chi^*(|F_{\text{env}}|)\}$ as input $u(t)$. It is not hard to obtain that

$$\nabla V(x_m(t))[g_\sigma(x_m) + h_\sigma(x_m)(\bar{F}_h + F_r)] \leq -\alpha_m(|x_m(t)|) + \gamma_m(|u_\sigma(t)|). \tag{37}$$

From (37), a common ISS Lyapunov triple function $(V_m, \alpha_m, \gamma_m)$ can be established. With V_m being smooth, it can be concluded that the system with switched control laws is uniformly ISS according to Theorem 3.1 given by Mancilla-Aguilar and Garc.[29]

Inequality (36) implies that subsystem (24) is ISS with respect to inputs $\bar{\zeta}_h$, $\bar{\psi}_h$, and $|F_{\text{env}}|$. This completes the proof of Lemma 1. □

Combining Lemma 1 with Theorem 1, a theorem about the stability of the master device subsystem with input F_h can be concluded.

https://doi.org/10.1017/S0263574714000800 Published online by Cambridge University Press

Theorem 2. The following master side subsystem,

$$\begin{cases} \dot{x}_m = g(x_m) + h(x_m)(F_h + F_r) \\ F_r = f_r(\bar{F}_h, F_{\text{env}}) \end{cases} \tag{38}$$

is ISS, with $f_r(\cdot)$ being the same as that in (24).

Proof. The input of the master device can be rewritten as

$$F_h + F_r = F_h - \bar{F}_h + \bar{F}_h + F_r. \tag{39}$$

Theorem 1 has pointed out that the estimation error $\left|F_h - \bar{F}_h\right|$ is bounded as $t \to \infty$. Specifically, we have

$$\left|F_h - \bar{F}_h\right| \leq \max\left\{\beta^*\left(\left|F_h(0) - \bar{F}_h(0)\right|, t\right), \gamma^*_{(\bar{\varepsilon})}\left(\sup_{t>0}|\bar{\varepsilon}(t)|\right), \gamma^*_{(F)}\left(\sup_{t\geq 0}\left|\dot{F}_h(t)\right|\right)\right\}. \tag{40}$$

The time derivative of the ISS Lyapunov function is

$$\begin{aligned} \dot{V}(x_m(t)) &:= \nabla V(x_m(t))\left[g(x_m) + h(x_m)(F_h + F_r)\right] \\ &= \nabla V(x_m(t))g(x_m) + \nabla V(x_m(t))h(x_m)(F_h - \bar{F}_h + \bar{F}_h + F_r) \\ &\leq \nabla V(x_m(t))g(x_m) + |\nabla V(x_m(t))h(x_m)|\,|F_h - \bar{F}_h| \\ &\quad + \nabla V(x_m(t))h(x_m)(\bar{F}_h + F_r). \end{aligned} \tag{41}$$

Using the fact that

$$\nabla V(x_m(t))g(x_m) + |\nabla V(x_m(t))h(x_m)|\,|u_m(t)| \leq -\alpha_m\left(|x_m(t)|\right) + \gamma_m\left(|u_m(t)|\right) \tag{42}$$

yields

$$\begin{aligned} &\nabla V(x_m(t))\left[g(x_m) + h(x_m)(F_h + F_r)\right] \\ &\quad \leq -\alpha_m\left(|x_m(t)|\right) + \gamma_m(\max\{2\left|F_h - \bar{F}_h\right|, 2\bar{\zeta}_h, 4\bar{\psi}_h, 2\chi^*(|F_{\text{env}}|)\}), \end{aligned} \tag{43}$$

where $|F_h - \bar{F}_h|$ satisfies inequality (40). Therefore, system (38) is ISS with respect to inputs as $|F_h(0) - \bar{F}_h(0)|$, $|\bar{\varepsilon}(t)|$, $|\dot{F}_h(t)|$, $\bar{\zeta}_h$, $\bar{\psi}_h$, and $|F_{\text{env}}|$. □

The next conclusion is about the stability of the closed-loop teleoperation system. Since the slave robot system is contained in the loop, an assumption about the local controller of the slave robot is given first.

Assumption 4. The slave robot system is IOS under the local controller with the IOS gain as γ_s.

The time delays existing in the communication are taken into account. Denote the input of the slave system as $u_s(t) : y_m(t - d_f(t))$ and the output of the slave system as $y_s(t) : f_{\text{env}}(t + d_b(t))$, where $d_f(t)$ and $d_b(t)$ are time delays in the forward and the backward channel. Under Assumption 4, the following conclusion could be obtained.

Theorem 3. The close-loop teleoperation system is ISS with respect to input as $\{|F_h(0) - \bar{F}_h(0)|, |\bar{\varepsilon}(t)|, |\dot{F}_h(t)|, |F_h^{\Xi}(t)|\}$ if the following small-gain stability condition can be satisfied,

$$\gamma_s \circ 2\chi^*(s) < \mathbb{I}(s) \quad \text{for all } s \in \mathbb{R}^+. \tag{44}$$

Proof. The output of the master side contains information of the master robot states. It is clear that the IOS gain from $|F_{\text{env}}|$ to the master output $y_m(t)$ is $2\chi^*$.

https://doi.org/10.1017/S0263574714000800 Published online by Cambridge University Press

Table I. Variation of $|F_r|$ during teleoperation.

	From/ To	Case (i)	Case (ii)	From/ To	Case (iii)	Case (iv)
$\left\|F_{\text{env}}^{\Xi}\right\| / \left\|\bar{F}_h^{\Xi}\right\| \leq 1$	Case (i)	Y[a]	Y	Case (iii)	Y	Y
	Case (ii)	Y	Y	Case (iv)	Y	Y
$\left\|F_{\text{env}}^{\Xi}\right\| / \left\|\bar{F}_h^{\Xi}\right\| > 1$	Case (i)	Y	N	Case (iii)	Y	N
	Case (ii)	N[b]	Y	Case (iv)	N	Y

[a]Y denotes smooth variation.
[b]N denotes possible jumps in $|F_r|$.

According to the multichannel small gain theorem,[30] the system is ISS if $\gamma_s \circ 2\chi^*(s) < \mathbb{I}(s)$, with the inputs $\{|F_h(0) - \bar{F}_h(0)|,\ |\bar{\varepsilon}(t)|,\ |\dot{\bar{F}}_h(t)|,\ \bar{\zeta}_h, \bar{\psi}_h\}$.

It is easy to see that $\bar{\zeta}_h(t) \leq |F_h^{\Xi}(t)| + |\bar{\zeta}_h(t) - F_h^{\Xi}(t)|$. Using the relationship between $\bar{F}_h(t)$ and $\bar{\zeta}_h(t)$, it can be derived that $|F_h^{\Xi}(t) - \bar{\zeta}_h(t)|$ is also bounded as

$$\begin{aligned}
&\left|F_h^{\Xi}(t) - \bar{\zeta}_h(t)\right| = \mu^* \left|F_h(t) - \bar{F}_h(t)\right| \\
&\leq \max\left\{\mu^* \circ \beta^*\left(\left|F_h(0) - \bar{F}_h(0)\right|, t\right), \mu^* \circ \gamma_{(\varepsilon)}^*\left(\sup_{t>0}|\bar{\varepsilon}(t)|\right),\ \mu^* \circ \gamma_{(\dot{F})}^*\left(\sup_{t\geq 0}\left|\dot{\bar{F}}_h(t)\right|\right)\right\}. \quad (45)
\end{aligned}$$

Therefore, the close-loop teleoperation system is ISS with the input as $\{|F_h(0) - \bar{F}_h(0)|, |\bar{\varepsilon}(t)|, |\dot{\bar{F}}_h(t)|, |F_h^{\Xi}(t)|\}$. This completes the proof. □

3.3. Haptic experience analysis

The quality of haptic experience is an important consideration in bilateral teleoperation. In the proposed scheme, the construction of the force reflection algorithm is piecewise. Therefore, the switching between different cases may cause jumps in the reflected force. In this section, the haptic experience is studied from two aspects, namely the magnitude and the direction of the reflected force.

It is more sensible to analyze the smooth of the reflected force on the premise that the human force F_h is maintained at a fixed value. This could be explained by the relationship of the action–reaction forces. When one is pushing against a wall, the reaction force will jump only when the action force changes suddenly. Therefore, we will analyze the way how the reflected force responds to the variations of the environment force.

Recalling Eq. (10), it can be seen that within each case, smooth variations of the environment force F_{env} will lead to smooth F_r. Here we will mainly focus on the continuity of the reflected force when switches happen. Since F_h is fixed, there are switches between cases (i) and (ii), and cases (iii) and (iv) respectively. In cases (ii) and (iii), the magnitude of the reflected force $|F_r|$ is only determined by F_{env}, while in cases (i) and (iv), $|F_r|$ is determined by F_h and F_{env}. To be specific, when $|F_{\text{env}}^{\Xi}|/|\bar{F}_h^{\Xi}| \leq 1$, $|F_r|$ in cases (i) and (iv) is only relevant to F_{env}. With a proper selection of χ_2 and χ_3, one can ensure the smooth variation of $|F_r|$ during switching between these four cases. When $|F_{\text{env}}^{\Xi}|/|\bar{F}_h^{\Xi}| > 1$, $|F_r|$ in cases (i) and (iv) is determined by $|F_h^{\Xi}|$ and F_{env}. Since F_h has the characteristic of randomness, choosing an appropriate χ_i to guarantee the continuity of $|F_r|$ is difficult. Another explanation of this result is that some degree of haptic experience is sacrificed for the stability of bilateral teleoperators. A performance matrix is given in Table I, which illustrates the smoothness of $|F_r|$ from one case to another. Table I indicates that in most cases, the smoothness of $|F_r|$ could be guaranteed, except for some few cases when system stability becomes a prime consideration.

One advantage of this method is the accurate direction of the reflected force. A recently proposed algorithm is introduced here for analysis, which is[15]

$$f_r = \frac{\alpha(|\hat{f}_{\text{env}}|)}{|\hat{f}_{\text{env}}|}\hat{f}_{\text{env}} + \frac{[\mathbb{I} - \alpha](|\hat{\phi}_{\text{env}}|)}{|\hat{\phi}_{\text{env}}|}\hat{\phi}_{\text{env}}. \quad (46)$$

In algorithm (46), $\hat{\phi}_{\text{env}}$ shares the same direction with $\hat{f}_h$. When $\hat{f}_{\text{env}}$ and $\hat{f}_h$ are not collinear, there is a bias between the directions of f_r and $\hat{f}_{\text{env}}$ unless the gain functional is selected as $\alpha(\cdot) = \mathbb{I}(\cdot)$. However,

https://doi.org/10.1017/S0263574714000800 Published online by Cambridge University Press

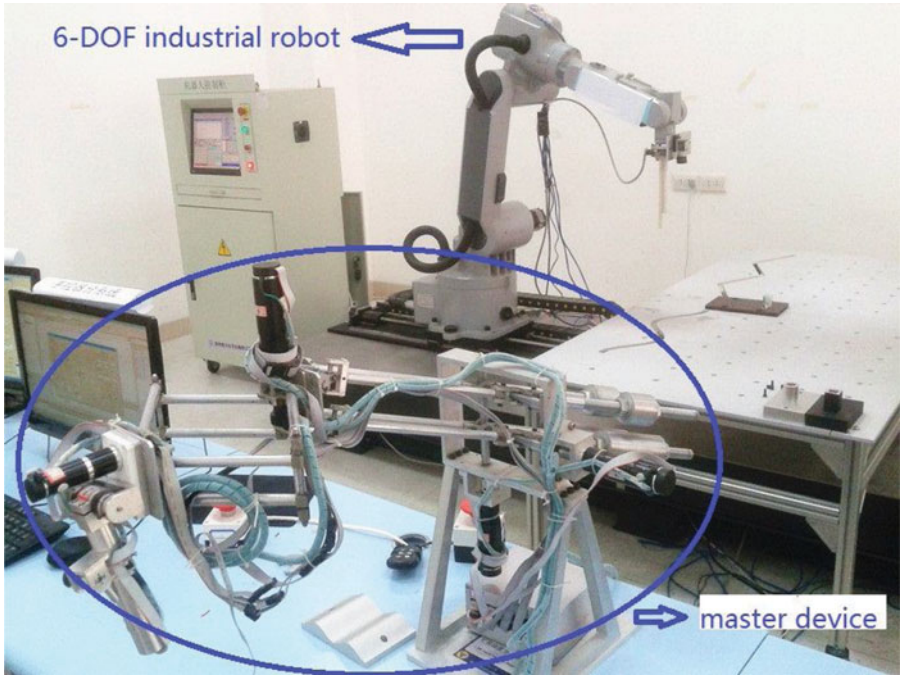

Fig. 2. Experiment setup.

if $\alpha(\cdot) = \mathbb{I}(\cdot)$, then algorithm turns into $f_r = \alpha(|\hat{f}_{\text{env}}|)\hat{f}_{\text{env}}/|\hat{f}_{\text{env}}|$, which means f_r is independent of f_h all the time and the stability criterion based on this algorithm will become conservative. In algorithm (10), it can be seen that in each case the direction of f_r always maintains the same as that of f_{env}. This implies that the direction of f_r varies smoothly during switches.

4. Simulations and Experiments

4.1. Experimental setup

The efficiency of the force reflection scheme is tested by simulations and ground teleoperation experiments. The experiments are performed on a 6-DOF teleoperation system. The system consists of a 7-DOF force feedback haptic device[31] as the master and a 6-DOF industrial robot as the slave. An ATI six-axis force/torque sensor Delta is located on the end-effectors of the slave robot, with the force signal sampling frequency as 1 kHz. The slave industrial robot is controlled by a host computer. Communication between the master and the slave is realized through the User Datagram Protocol (UDP) Ethernet. The experiment platform is shown in Fig. 2.

4.2. Experiment results

Because the haptic device is not equipped with a force sensor, first *s* simulation is performed to validate the human force estimation algorithm. A two-link manipulator is considered in the simulation. The dynamics is as Eq. (1), and the parameter matrices are

$$M(q) = \begin{bmatrix} 6.733 + 6\cos q_2 & 3.4 + 6\cos q_2 \\ 3.4 + 6\cos q_2 & 3.4 \end{bmatrix} \quad C(q, \dot{q}) = \begin{bmatrix} -6\dot{q}_2 \sin q_2 & -3\dot{q}_2 \sin q_2 \\ 3\dot{q}_1 \sin q_2 & 0 \end{bmatrix}.$$

The length of links are $l_1 = 1$, $l_2 = 2$. In the initial state, the joint angles of the manipulator are zero, and the position of the end point is [3 0 0]. The operator imposes on the end of the manipulator and intends to pull the end to the position [1.7758 2.3457 0]. Besides the human force, there are also control torques exerted on the manipulator.

The choosing of α in (5) has a significant effect on force estimation. α determines the cut-off frequency of the low pass filter (3). If the value of α is too high ($\alpha > 1$), the lag of the estimates will

https://doi.org/10.1017/S0263574714000800 Published online by Cambridge University Press

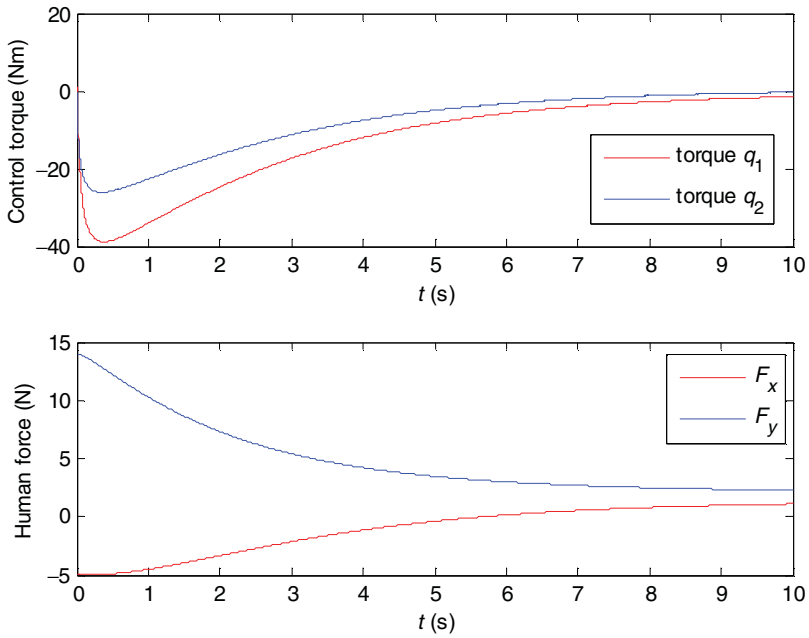

Fig. 3. Torques and forces imposed on the robot.

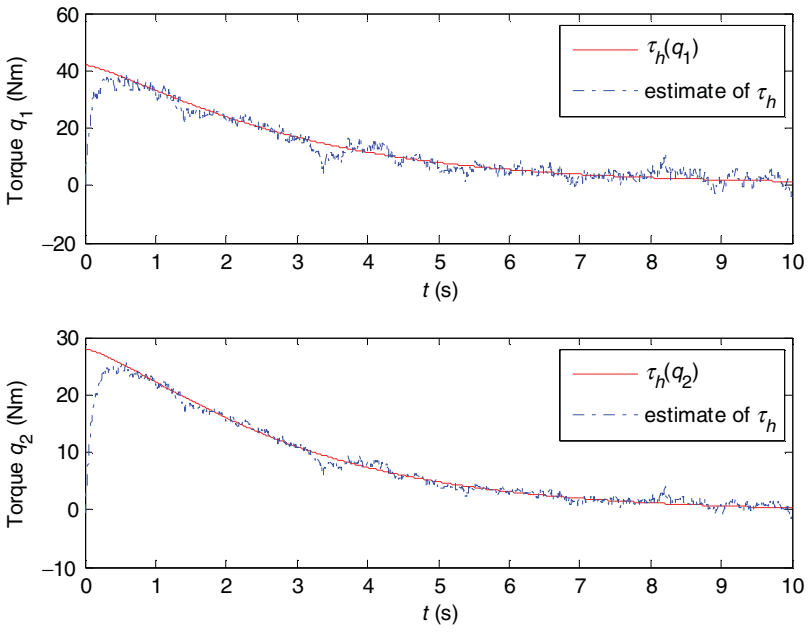

Fig. 4. Estimates of human forces.

be distinct, and the estimation errors in initial state will last for a long time (Theorem 1 also implies that the error bound will increase with greater α). Otherwise, if α is too small, the filter is with a high cut-off frequency. As mentioned above, the frequency of the human operator is up to 10 Hz. Hence, in this case high frequency noises will be introduced into the estimates. In our simulations, the parameter is selected as $\alpha = 0.1$, corresponding to a cut-off frequency of 10 Hz. Gaussian white noises with variance as 1e-3 are added into the measure of joint velocities. The control torques and human forces applied on the end of the manipulator are shown in Fig. 3. The estimates of the real torques are shown in Fig. 4. The estimate errors with different values of α are shown in Fig. 5. It could be seen in Fig. 5 that $\alpha = 0.1$ is an appropriate choice based on an overall analysis of accuracy and convergence.

https://doi.org/10.1017/S0263574714000800 Published online by Cambridge University Press

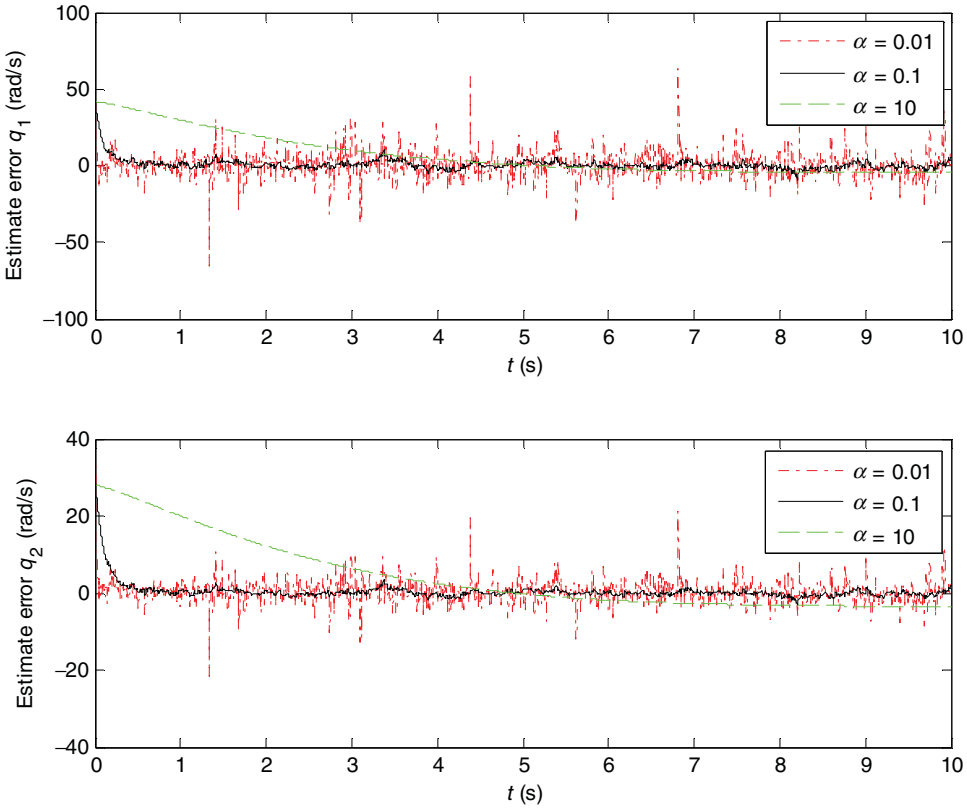

Fig. 5. Estimate errors with different values of α.

Two experiments are carried out to evaluate the method proposed in this paper. For the convenience of data analysis, the end-effector of the slave robot moves only in the horizontal plane, which is also the x–y plane of the base Cartesian coordinate.

In the first experiment, the end-effector of the slave robot is initially at rest in the free space without any contact. Then the human operator moves the end of the master along a specific direction until the end-effector of the slave robot hits a line obstacle, where the slave robot will be pushed back by a contact force. The line obstacle is along with the y-direction, and hence the contact force is mainly in the x-direction. The location of the obstacle in the base Cartesian coordinate is $y = 0.94$. The input of the slave robot system is the velocity of the master end-effector, with the scaling as 0.2, i.e., $u_s(t) = 0.2y_m(t) = 0.2v_m(t)$. The velocities of the master and slave robots are shown in Fig. 6.

It can be seen in Fig. 6 that the end-effector of the slave moves in the free space when $t < 23$ s. At time $t = 23$ s, the tool hits the obstacle and the movement along the x-direction is hampered. Note that there is still a non-zero velocity in the x-direction after the contact happens. This is because the end tool is elastic, and twist would happen so that the velocity of the tool center point (TCP) is not zero even if the top point of the tool is fixed. During the experiment, there are three instances when the velocity in the x-direction reduces to zero. These instances are when the work zone of the master is re-adjusted.

The contact force measured by the force sensor and the reflected force is shown in Fig. 7.

It could be found that the trend of the reflected force is compatible with the contact force. In the free move stage, the contact force mostly remains at zero, with a noise of less than 0.5 N. There are some tiny oscillations in the slave end force during the acceleration phases because of the inertia effect, but these are not clearly felt by human operator as these are much smaller than the human force. At the beginning of the contact stage, the reflected force is the same as the contact force. As the contact force increases, over-high reflected forces would break the stability of teleoperators, so the reflected force is reproduced via the orthogonal decomposition of the contact force according to the human force and the velocity of the master. It is demonstrated in Fig. 7 that at this point, the reflected force is lower than the contact force, but can still express the trend of the contact force. The

https://doi.org/10.1017/S0263574714000800 Published online by Cambridge University Press

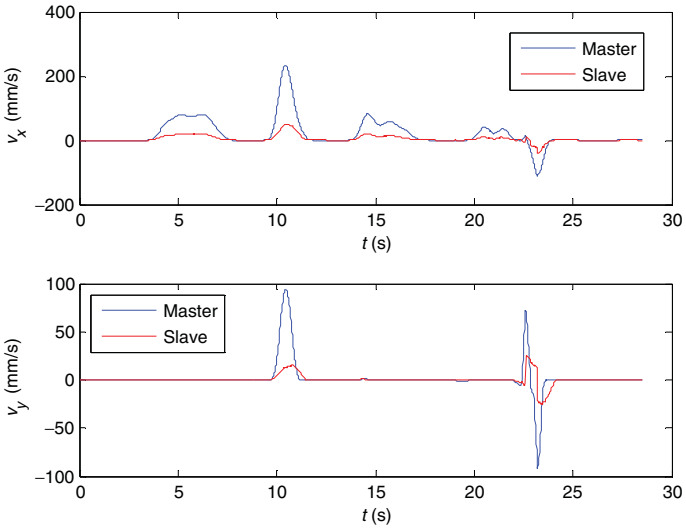

Fig. 6. Velocities of slave and master robots.

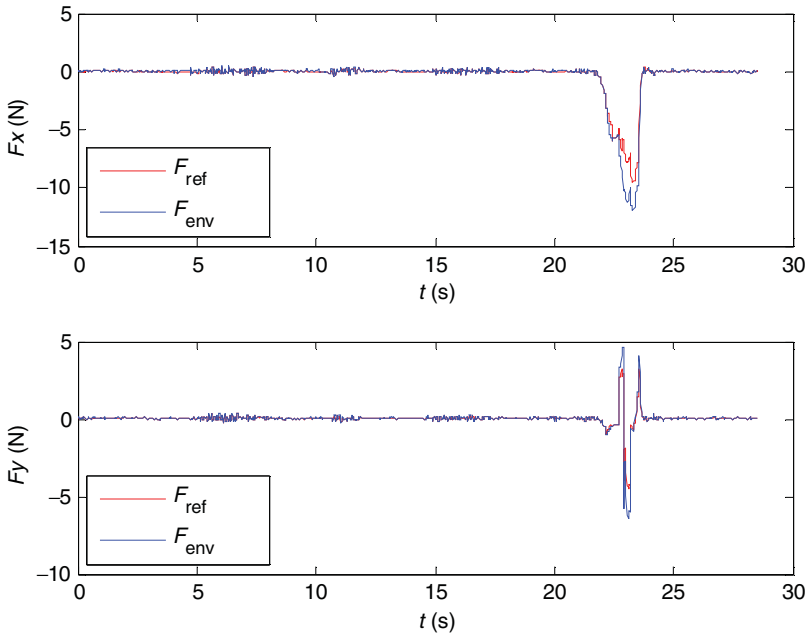

Fig. 7. Reflected force in x- and y-directions.

force in the y-direction is the friction force when the human operator briefly shakes the master after the contact happens. The estimated human force is shown in Fig. 8.

The second set of experiments is a curvilinear groove tracking task, which is a typical guiding contact task. In the experiment, the slave end-effector is controlled to slide in the curvilinear groove (Fig. 9). The human operator moves the master based on the reflected force he feels. Unlike the first experiment, in this case the contact force always exists during the movement of the slave robot. In addition, in order to testify the stability of teleoperation under time delay, a round-trip delay of about 2 s is introduced into the transmission channel.

There would be no drastic impact force imposed on the end-effector during this experiment, so a higher velocity scaling is chosen. The scaling is set as 0.5, i.e., $u_s(t) = 0.2y_m(t) = 0.2v_m(t)$. The force and the velocity of TCP are shown in Fig. 10.

As is shown in Fig. 10, the reflected force in this experiment follows the contact force more closely than in the first experiment. There are two reasons accounting for this. First, the contact force is lower

https://doi.org/10.1017/S0263574714000800 Published online by Cambridge University Press

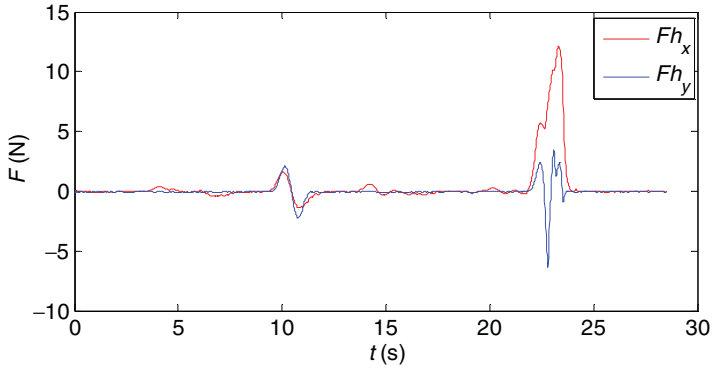

Fig. 8. Estimates of human force.

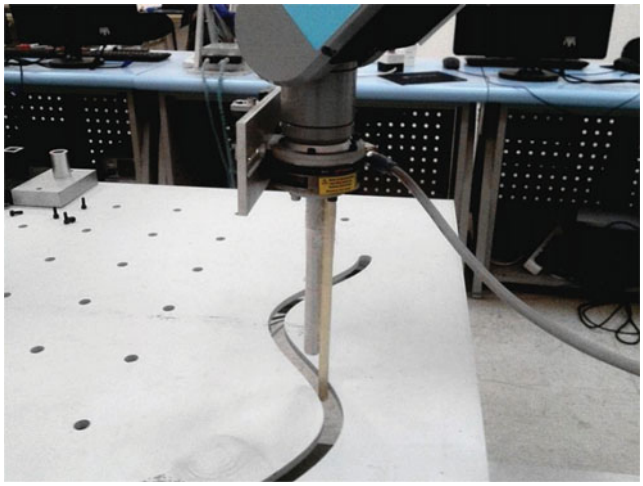

Fig. 9. Curvilinear groove

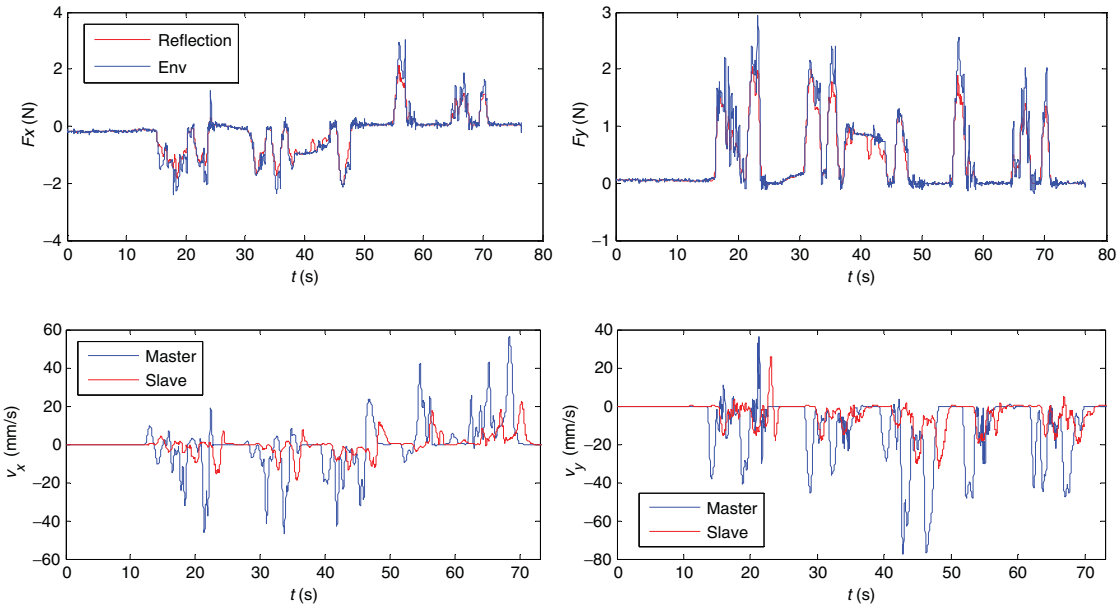

Fig. 10. Reflected forces and velocity curves.

https://doi.org/10.1017/S0263574714000800 Published online by Cambridge University Press

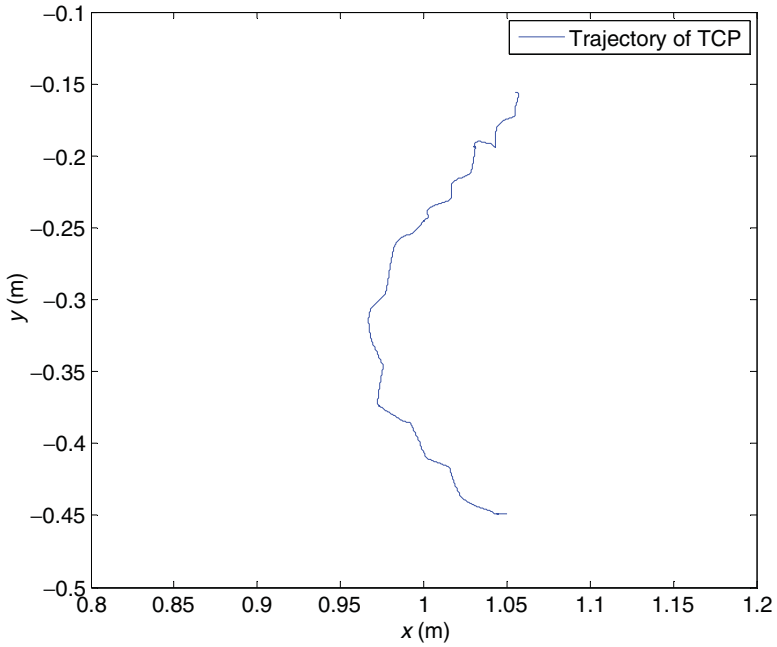

Fig. 11. The trajectory of the slave TCP.

than the impact force in the former experiment, thus the human operator could handle the master under the contact force. Second, the contact force is mainly the friction force in this experiment. As is known to us, the friction force dissipates energy and brings damping effect for the system. Therefore, the friction force F_{fri} always satisfies $F_{\text{fri}} \in \Theta$. Algorithm (10) and Lemma 1 suggest that in this case the gain $\chi_2(\cdot)$ or $\chi_3(\cdot)$ has no influence on stability. Hence, in the experiments both gains $\chi_2(\cdot)$ and $\chi_3(\cdot)$ are set to be the constant 1 in order to obtain a better telepresence, which means that the reflected forces are equal to the contact force in this case.

Due to the existence of time delays, there is a lag between the response of the slave robot and the command of the master, as shown in Fig. 10 (the velocities curve). It could be seen that the teleoperators still remain stable under time delays during the whole experiment.

In order to illustrate the superiority of the proposed method, especially its advantage in direction rendering, a contrast is made between the proposed adaptive force reflection scheme and a traditional projection-based force reflection algorithm.[15] The directions of the contact force (measured by the force sensor) and the reflected force generated by the traditional algorithm and the proposed algorithm are given in Fig. 12. The results show that using the proposed method, the reflected force is in the same direction as the contact force. In the traditional approach, deviations exist between the contact force and the reflected force. The deviation in the direction reaches up to about 60°, which degrades telepresence and can be misleading for operators.

Overall, both sets of experiments demonstrate that the force reflection algorithm exhibits good telepresence and effectively helps the human operator to accomplish the tasks.

5. Conclusions

A novel adaptive force reflection scheme for bilateral teleoperation is presented in this paper. In order to achieve the best telepresence performance and, at the same time, to ensure the stability of the teleoperation system, the force reflection algorithm is designed based on an overall analysis of the human force and the contact force. The human force is estimated via an observer, which is designed according to the characteristic of human operation. The convergence of the observing errors can be guaranteed in the presence of measurement noises. With the aid of the concepts, such as the passive and non-passive regions, the relationship between the contact force and the human action is analyzed in detail, which becomes the basis of the reflection algorithm. So far, as is known to the authors, no similar research has been conducted in the existing area. The reflected force is based on the orthogonal

https://doi.org/10.1017/S0263574714000800 Published online by Cambridge University Press

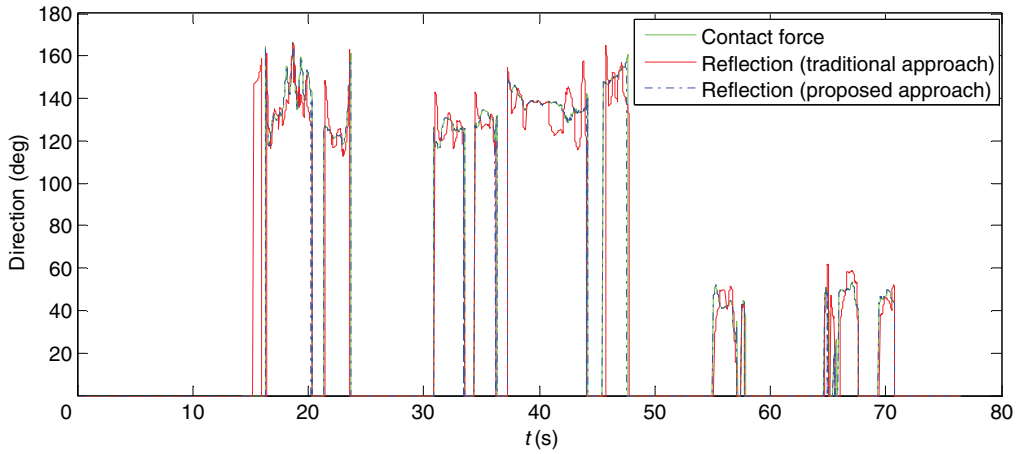

Fig. 12. Directions of the forces.

complement of the contact force measured by the force sensor mounted on the end of the slave robot. The reflected force is adaptively adjusted according to the estimated human force to eliminate non-passive IMMs. In this way the stability of bilateral teleoperators is ensured. The Teleoperation with the designed reflected force is proved to be stable using the small-gain theorem. Compared with the traditional algorithm, a lower conservative stability criterion is derived. The effects on haptic experience are discussed from the magnitude and direction of the reflected force. In most cases, the smoothness of the magnitude can be guaranteed. The accuracy of the direction can be always ensured during the teleoperation, which indicates the superiority of this scheme in the guiding contact task.

The results of simulations and experiments confirm the effectiveness of the proposed scheme. The simulations demonstrate the validity of the human force estimation algorithm. It is shown in the experiments that the force reflection helps the human operator finish the operations successfully, and the stability of the teleoperation is also guaranteed during the tasks. The claimed superiority of the force reflection scheme is validated in the contrast experiment. The method reduces dependency on the human–master interaction dynamic model and relaxes assumptions about the passivity of human action, so it possesses more universal applicable value in practice.

Acknowledgements

This research is supported by the National Natural Science Foundation of China (Grant no. 61175098) and Shenzhen Basic Research Project (Grant no. JCYJ20130401171935812). The authors would like to thank the anonymous reviewers for their comments which greatly help to improve the contents of this paper.

References

1. T. B. Sheridan, "Telerobotics," *Automatica* **25**(4), 487–507 (1989).
2. G. Niemeyer, C. Preusche and G, Hirzinger, "Telerobotics," **In:** *Springer Handbook of Robotics* (Springer, New york, NY, 2008) pp. 741–757.
3. C. Passenberg, A. Peer and M. Buss, "A survey of environment-, operator-, and task-adapted controllers for teleoperation systems." *Mechatronics* **20**(7), 787–801 (2010).
4. D. A. Lawrence, "Stability and transparency in bilateral teleoperation," *IEEE Trans. Robot. Autom.* **9**(5), 624–637 (1993).
5. K. Hashtrudi-Zaad and S. E. Salcudean, "Transparency in time-delayed systems and the effect of local force feedback for transparent teleoperation," *IEEE Trans. Robot. Autom.* **18**(1), 108–114 (2002).
6. E. Nuño, L. Basañez and R. Ortega, "Passivity-based control for bilateral teleoperation: A tutorial," *Automatica* **47**(3), 485–495 (2011).
7. R. J. Anderson and M. W. Spong, "Bilateral control of teleoperators with time delay," *IEEE Trans. Autom. Control* **34**(5), 494–501 (1989).
8. G. Niemeyer and J. J. E. Slotine, "Stable adaptive teleoperation," *IEEE J. Ocean. Eng.* **16**(1), 152–162 (1991).

https://doi.org/10.1017/S0263574714000800 Published online by Cambridge University Press

9. J. H. Park and H. C. Cho, "Sliding Mode Control of Bilateral Teleoperation Systems with Force-Reflection on the Internet," *Proceedings of the 2000 IEEE/RSJ International Conference on Intelligent Robots and Systems (IROS 2000)* (2000) pp. 1187–1192.
10. J. Yan and S. E. Salcudean, "Teleoperation controller design using H_∞-optimization with application to motion-scaling," *IEEE Trans. Control Syst. Technol.* **4**(3), 244–258 (1996).
11. G. M. H. Leung, B. A. Francis and J. Apkarian, "Bilateral controller for teleoperators with time delay via μ -synthesis," *IEEE Trans. Robot. Autom.* **11**(1), 105–116 (1995).
12. P. F. Hokayem and M. W. Spong, "Bilateral teleoperation: An historical survey," *Automatica* **42**(12), 2035–2057 (2006).
13. R. W. Daniel and P. R. McAree, "Fundamental limits of performance for force reflecting teleoperation," *Int. J. Robot. Res.* **17**(8), 811–830 (1998).
14. K. J. Kuchenbecker and G. Niemeyer, "Induced master motion in force-reflecting teleoperation," *J. Dyn. Syst. Meas. Control* **128**(4), 800–810 (2006).
15. I. G. Polushin, X. P. Liu and C. Lung, "Stability of bilateral teleoperators with generalized projection-based force reflection algorithms," *Automatica* **48**(6), 1005–1016 (2012).
16. K. J. Kuchenbecker, J. Fiene and G. U. N. Niemeyer, "Event-Based Haptics and Acceleration Matching: Portraying and Assessing the Realism of Contact," *First Joint Eurohaptics Conference and Symposium on Haptic Interfaces for Virtual Environment and Teleoperator Systems*, Pisa, Italy (2005) pp. 381–387.
17. B. T. Gleeson, S. K. Horschel and W. R. Provancher, "Perception of direction for applied tangential skin displacement: Effects of speed, displacement, and repetition," *IEEE Trans. Haptics* **3**(3), 177–188 (2010).
18. H. Kawasaki, Y. Ohtuka, S. Koide and T. Mouri, "Perception and haptic rendering of friction moments," *IEEE Trans. Haptics* **4**(1), 28–38 (2011).
19. H. K. Khalil, *Nonlinear Systems* (Prentice Hall, Upper Saddle River, NJ, 2002).
20. A. R. Teel, "Connections between Razumikhin-type theorems and the ISS nonlinear small gain theorem," *IEEE Trans. Autom. Control* **43**(7), 960–964 (1998).
21. M. W. Spong, S. Hutchinson and M. Vidyasagar, *Robot Modeling and Control* (John Wiley, New York, NY, 2006).
22. N. A. Tanner and G. Niemeyer, "High-frequency acceleration feedback in wave variable telerobotics," *IEEE/ASME Trans. Mechatronics* **11**(2), 119–127 (2006).
23. A. Stotsky and I. Kolmanovsky, "Application of input estimation techniques to charge estimation and control in automotive engines," *Control Eng. Pract.* **10**(12), 1371–1383 (2002).
24. I. Kolmanovsky, I. Sivergina and J. Sun, "Simultaneous input and parameter estimation with input observers and set-membership parameter bounding: Theory and an automotive application," *Int. J. Adapt. Control* **20**(5), 225–246 (2006).
25. A. L. Fradkov, I. V. Miroshnik and V. O. Nikiforov, *Nonlinear and Adaptive Control of Complex Systems* (Springer, New York, NY, 1999).
26. E. D. Sontag and Y. Wang, "Notions of input to output stability," *Syst. Control Lett.* **38**(4), 235–248 (1999).
27. E. Sontag, "Input to State Stability: Basic Concepts and Results," **In:** *Nonlinear and Optimal Control Theory* (Springer-Verlag, Berlin, Germany, 2008) 163–220.
28. I. G. Polushin, P. X. Liu and L. Chung-Horng, "A force-reflection algorithm for improved transparency in bilateral teleoperation with communication delay," *IEEE/ASME Trans. Mechatronics* **12**(3), 361–374 (2007).
29. J. L. Mancilla-Aguilar and R. A. Garc, "On converse Lyapunov theorems for ISS and iISS switched nonlinear systems," *Syst. Control Lett*. **42**(1), 47–53 (2001).
30. I. Polushin, H. J. Marquez, A. Tayebi and P. X. Liu, "A multichannel IOS small gain theorem for systems with multiple time-varying communication delays," *IEEE Trans. Autom. Control* **54**(2), 404–409 (2009).
31. W. Jianfeng, S. Aiguo and L. Jianqing, "A three-dimensional force reflecting hand controller," *Chin. J. Sens. Actuators* **23**, 1417–1420 (2010).